Maximizing the information learned from finite data selects a simple model

Henry H. Mattingly[a], **Mark K. Transtrum**[b], **Michael C. Abbott**[c,1], **and Benjamin B. Machta**[d,1]

[a]Lewis-Sigler Institute and Department of Chemical and Biological Engineering, Princeton University, Princeton, NJ 08544, USA; [b]Department of Physics and Astronomy, Brigham Young University, Provo, Utah 84602, USA; [c]Marian Smoluchowski Institute of Physics, Jagiellonian University, Ulica Łojasiewicza 11, 30-348 Kraków, Poland; [d]Lewis-Sigler Institute and Department of Physics, Princeton University, Princeton, NJ 08544, USA

We use the language of uninformative Bayesian prior choice to study the selection of appropriately simple effective models. We advocate for the prior which maximizes the mutual information between parameters and predictions, learning as much as possible from limited data. When many parameters are poorly constrained by the available data, we find that this prior puts weight only on boundaries of the parameter manifold. Thus it selects a lower-dimensional effective theory in a principled way, ignoring irrelevant parameter directions. In the limit where there is sufficient data to tightly constrain any number of parameters, this reduces to Jeffreys prior. But we argue that this limit is pathological when applied to the hyper-ribbon parameter manifolds generic in science, because it leads to dramatic dependence on effects invisible to experiment.

Effective Theory | Model Selection | Renormalization Group | Bayesian Prior Choice | Information Theory

Physicists prefer simple models not because nature is simple, but because most of its complication is usually irrelevant. Our most rigorous understanding of this idea comes from the Wilsonian renormalization group (1–3), which describes mathematically the process of zooming out and losing sight of microscopic details. These details only influence the effective theory which describes macroscopic observables through a few relevant parameter combinations, such as the critical temperature, or the proton mass. The remaining irrelevant parameters can be ignored, as they are neither constrained by past data nor useful for predictions. Such models can now be understood as part of a large class called sloppy models (4–14), whose usefulness relies on a similar compression of a large microscopic parameter space down to just a few relevant directions.

This justification for model simplicity is different from the one more often discussed in statistics, motivated by the desire to avoid overfitting (15–21). Since irrelevant parameters have an almost invisible effect on predicted data, they cannot be excluded on these grounds. Here we motivate their exclusion differently: we show that simplifying a model can often allow it to extract more information from a limited data set, and that this offers a guide for choosing appropriate effective theories.

We phrase the question of model selection as part of the choice of a Bayesian prior on some high-dimensional parameter space. In a set of nested models, we can always move to a simpler model by using a prior which is nonzero only on some subspace. Recent work has suggested that interpretable effective models are typically obtained by taking some parameters to their limiting values, often 0 or ∞, thus restricting to lower-dimensional boundaries of the parameter manifold (22).

Our setup is that we wish to learn about a theory by performing some experiment which produces data $x \in X$.

The theory and the experiment are together described by a probability distribution $p(x|\theta)$, for each value of the theory's parameters $\theta \in \Theta$. This function encodes both the quality and quantity of data to be collected.

The mutual information between the parameters and their expected data is defined as $\mathrm{MI} = I(X;\Theta) = S(\Theta) - S(\Theta|X)$, where S is the Shannon entropy (23). The MI thus quantifies the information which can be learned about the parameters by measuring the data, or equivalently, the information about the data which can be encoded in the parameters (24, 25). Defining $p_\star(\theta)$ by maximizing this, we see:

i. The prior $p_\star(\theta)$ is almost always discrete (26–30), with weight only on a finite number K of points, or atoms (Figures 1 and 2): $p_\star(\theta) = \sum_{a=1}^{K} \lambda_a \delta(\theta - \theta_a)$.

ii. When data is abundant, $p_\star(\theta)$ approaches Jeffreys prior $p_{\mathrm{J}}(\theta)$ (31–33). As this continuum limit is approached, the proper spacing of the atoms shrinks as a power law (Figure 3).

iii. When data is scarce, most atoms lie on boundaries of parameter space, corresponding to effective models with fewer parameters (Figure 4). The resulting distribution of weight along relevant directions is much more even than that given by Jeffreys prior (Figure 5).

Significance Statement

Most physical theories are effective theories, descriptions at the scale visible to our experiments which ignore microscopic details. Seeking general ways to motivate such theories, we find an information theory perspective: if we select the model which can learn as much information as possible from the data, then we are naturally led to a simpler model, by a path independent of concerns about overfitting. This is encoded as a Bayesian prior which is nonzero only on a subspace of the original parameter space. We differ from earlier prior selection work by not considering infinitely much data. Having finite data is always a limit on the resolution of an experiment, and in our framework this selects how complicated a theory is appropriate.
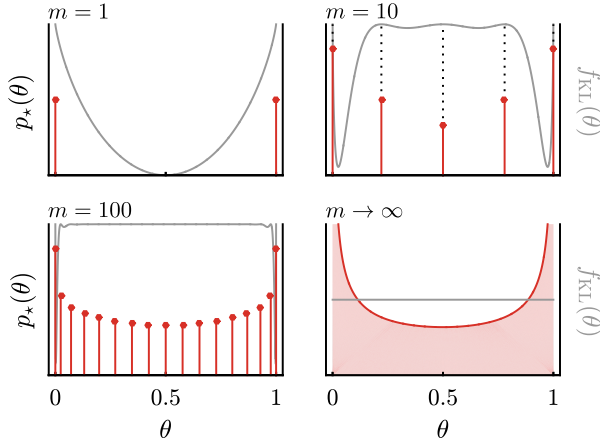
Fig. 1. Optimal priors for the Bernoulli model (1). Red lines indicate the positions of delta functions in $p_\star(\theta)$, which are at the maxima of $f_{\mathrm{KL}}(\theta)$, Eq. (3). As $m \to \infty$ these coalesce into Jeffreys prior $p_{\mathrm{J}}(\theta)$.

After some preliminaries, we demonstrate these properties in three simple examples, each a stylized version of a realistic experiment. To see the origin of discreteness, we study the bias of an unfair coin and the value of a single variable corrupted with Gaussian noise. To see how models of lower dimension arise, we then study the problem of inferring decay rates in a sum of exponentials.

In the Appendix we discuss the alorithms used for finding $p_\star(\theta)$ (Figures 2 and S3), and we apply some more traditional model selection tools to the sum of exponentials example (Figure S1).

Priors and Geometry

Bayes' theorem tells us how to update our knowledge of θ upon observing data x, from prior $p(\theta)$ to posterior $p(\theta|x) = p(x|\theta)p(\theta)/p(x)$, where $p(x) = \int d\theta\, p(\theta)\, p(x|\theta)$. In the absence of better knowledge we must pick an uninformative prior which codifies our ignorance. The naive choice of a flat prior $p(\theta) = $ const. has undesirable features, in particular making $p(x)$ depend on the choice of parameterization, through the measure $d\theta$.

Jeffreys prior $p_{\mathrm{J}}(\theta)$ is invariant under changes of parameterizaion, because it is constructed from some properties of the experiment (34). This $p_{\mathrm{J}}(\theta) \propto \sqrt{\det g_{\mu\nu}}$ is, up to normalization, the volume form arising from the Fisher information metric (FIM, often -matrix):

$$g_{\mu\nu}(\vec{\theta}) = \int dx\, p(x|\vec{\theta})\, \frac{\partial \log p(x|\vec{\theta})}{\partial \theta^\mu}\, \frac{\partial \log p(x|\vec{\theta})}{\partial \theta^\nu}.$$

This Riemannian metric defines a reparameterization-invariant distance between points, $ds^2 = \sum_{\mu,\nu=1}^{D} g_{\mu\nu}\, d\theta^\mu d\theta^\nu$. It measures the distinguishability of the data which θ and $\theta + d\theta$ are expected to produce, in units of standard deviations. Repeating an (identical and independently distributed) experiment m times means considering $p^m(\vec{x}|\theta) = \prod_{j=1}^{m} p(x_j|\theta)$, which leads to metric $g_{\mu\nu}^m(\theta) = m\, g_{\mu\nu}(\theta)$. However the factor $m^{D/2}$ in the volume is lost by normalizing $p_{\mathrm{J}}(\theta)$. Thus Jeffreys prior depends on the type of experiment, but not the quantity of data.

Bernardo defined a prior $p_\star(\theta)$ by maximizing the mutual information between parameters Θ and the expected data X^m from m repetitions, and then a reference prior by taking the limit $m \to \infty$ (29, 31). Under certain benign assumptions, this reference prior is exactly Jeffreys prior (31–33), providing an alternative justification for $p_{\mathrm{J}}(\theta)$.

We differ in taking seriously that the amount of data collected is always finite.[*] Besides being physically unrealistic, the limit $m \to \infty$ is pathological both for model selection and prior choice. In this limit any number of parameters can be perfectly inferred, justifying an arbitrarily complicated model. In addition, in this limit the posterior $p(\theta|x)$ becomes independent of any smooth prior.[†]

Geometrically, the defining feature of sloppy models is that they have a parameter manifold with hyper-ribbon structure (6–9): there are some long directions (corresponding to d relevant, or stiff, parameters) and many shorter directions ($D - d$ irrelevant, or sloppy, parameter combinations). These lengths are often estimated using the eigenvalues of $g_{\mu\nu}$, and have logarithms that are roughly evenly-spaced over many orders of magnitude (4, 5). The effect of coarse-graining is to shrink irrelevant directions (here using the technical meaning of irrelevant: a parameter which shrinks under renormalization group flow) while leaving relevant directions extended, producing a sloppy manifold (8, 14). By contrast the limit $m \to \infty$ has the effect of expanding all directions, thus erasing the distinction between directions longer and shorter than the critical length scale of (approximately) one standard deviation.

On such a hyper-ribbon, Jeffreys prior has an undesirable feature: since it is constructed from the D-dimensional notion of volume, its weight along the relevant directions always depends on the volume of the $D - d$ irrelevant directions. This gives it extreme dependence on which irrelevant parameters are included in the model.[‡] The optimal prior $p_\star(\theta)$ avoids this dependence because it is almost always discrete, at finite m.[§] It puts weight on a set of nearly distinguishable points, closely spaced along the relevant directions, but ignoring the irrelevant ones. Yet being the solution to a reparameterization-invariant optimization problem, the prior $p_\star(\theta)$ retains this good feature of $p_{\mathrm{J}}(\theta)$.

Maximizing the mutual information was originally done to calculate the capacity of a communication channel, and we can borrow techniques from rate-distortion theory here: the algorithms we use were developed there (37, 38), and the discreteness we exploit was discovered several times in engineering (26–28, 39). In statistics, this problem is more often discussed as an equivalent minimax problem (40). Discreteness was

---

[*]Interned for five years, John Kerrich only flipped his coin 10^4 times (35). With computers we can do better, but even the LHC only generated about 10^{18} bits of data (36).

[†]For simplicity we consider only regular models, i.e. we assume all parameters are structurally identifiable.

[‡]See Figure 5 for a demonstration of this point. For another example, consider a parameter manifold Θ which is a cone, with Fisher metric $ds^2 = (50\, d\vartheta)^2 + \vartheta^2 d\Omega_n^2/4$: there is one relevant direction $\vartheta \in [0, 1]$ of length $L = 50$, and n irrelevant directions forming a sphere of diameter ϑ. Then the prior on ϑ alone implied by $p_{\mathrm{J}}(\vec{\theta})$ is $p(\vartheta) = (n + 1)\vartheta^n$, putting most of the weight near to $\vartheta = 1$, dramatically so if $n = D - d$ is large. But since only the relevant direction is visible to our experiment, the region $\vartheta \approx 0$ ought to be treated similarly to $\vartheta \approx 1$. The prior $p_\star(\vec{\theta})$ has this property.

[§]We offer both numerical and analytic arguments for discreteness below. The exception to discreteness is that if there is an exact continuous symmetry, $p_\star(\theta)$ will be constant along it. For example if our Gaussian model Eq. (2) is placed on a circle (identifying both $\theta \sim \theta + 1$ and $x \sim x + 1$) then the optimum prior is a constant.

also observed in other minimax problems (41–43), and later in directly maximising mutual information (29, 30, 33, 44). However it does not seem to have been seen as useful, and none of these papers explicitly find discrete priors in dimension $D > 1$, which is where we see attractive properties. Discreteness has been useful, although for different reasons, in the idea of rational inattention in economics (45, 46). There, market actors have a finite bandwidth for news, and this drives them to make discrete choices despite all the dynamics being continuous. Rate-distortion theory has also been useful in several areas of biology (47–49), and discreteness emerges in a recent theoretical model of the immune system (50).

We view this procedure of constructing the optimal prior as a form of model selection, picking out the subspace of Θ on which $p_\star(\theta)$ has support. This depends on the likelihood function $p(x|\theta)$ and the data space X, but not on the observed data x. In this regard it is closer to Jeffreys' perspective on prior selection than to tools like the information criteria and Bayes factors, which are employed at the stage of fitting to data. We discuss this difference at more length in the Appendix.

One-Parameter Examples

We begin with some problems with a single bounded parameter, of length L in the Fisher metric. These tractable cases illustrate the generic behaviour along either short (irrelevant) or long (relevant, $L \gg 1$) parameter directions in higher-dimensional examples.

Our first example is the Bernoulli problem, in which we wish to determine the probability $\theta \in [0, 1]$ that an unfair coin gives heads, using the data from m trials. It is sufficient to record the total number of heads x, which occurs with probability

$$p(x|\theta) = \frac{m!}{x!(m-x)!}\, \theta^x (1-\theta)^{m-x}. \qquad [1]$$

This gives $g_{\theta\theta} = \frac{m}{\theta(1-\theta)}$, thus $p_J(\theta) = [\pi\sqrt{\theta(1-\theta)}]^{-1}$, and proper parameter space length $L = \int \sqrt{ds^2} = \pi\sqrt{m}$.

In the extreme case $m = 1$, the optimal prior is two delta functions, $p_\star(\theta) = \frac{1}{2}\delta(\theta) + \frac{1}{2}\delta(\theta - 1)$, and MI $= \log 2$, exactly one bit (29, 30, 33). Before an experiment that will only ever be run once, this places equal weight on both outcomes; afterwards it records the outcome. As m increases, weight is moved from the boundary onto interior points, which increase in number, and ultimately approach the smooth $p_J(\theta)$: see Figures 1 and 2A.

Similar behavior is seen in a second example, in which we measure one real number x, normally distributed with known σ about the parameter $\theta \in [0, 1]$:

$$p(x|\theta) = \frac{1}{\sqrt{2\pi}\sigma} e^{-(x-\theta)^2/2\sigma^2}. \qquad [2]$$

Repeated measurements are equivalent to smaller σ (by $\sigma \to \sigma/\sqrt{m}$), so we fix $m = 1$ here. The Fisher metric is $g_{\theta\theta} = 1/\sigma^2$, thus $L = 1/\sigma$. An optimal prior is shown in Figure 2, and in Figure 5A along with its implied distribution of expected data. This $p(x)$ is similar to that implied by Jeffreys prior, here $p_J(\theta) = 1$.

We calculated $p_\star(\theta)$ numerically in two ways. After discretizing both θ and x, we can use the Blahut–Arimoto (BA)
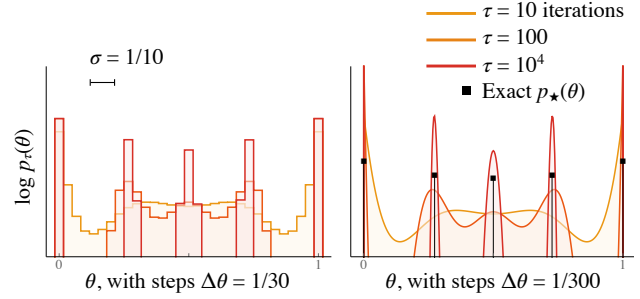

Fig. 2. Convergence of the Blahut–Arimoto algorithm. This is for the one-parameter Gaussian model Eq. (2) with $L = 10$ (comparable to $m = 10$ in Figure 1). On the right θ is discretized into ten times as many points, but $p_\tau(\theta)$ clearly converges to the same five delta functions.

algorithm (37, 38). This converges to the global maximum, which is a discrete distribution: see Figure 2. Alternatively, using our knowledge that $p_\star(\theta)$ is discrete, we can instead adjust the positions θ_a and weights λ_a of a finite number of atoms. See the Supplement for more details.

To see analytically why discreteness arises, we write the mutual information as

$$\text{MI} = I(X; \Theta) = \int d\theta\, p(\theta)\, f_{\text{KL}}(\theta), \qquad [3]$$

$$f_{\text{KL}}(\theta) = D_{\text{KL}}\big[p(x|\theta)\big\|p(x)\big] = \int dx\, p(x|\theta)\, \log\frac{p(x|\theta)}{p(x)}$$

where D_{KL} is the Kullback–Leibler divergence.¶ Maximizing MI over all functions $p(\theta)$ with $\int d\theta\, p(\theta) = 1$ gives $f_{\text{KL}}(\theta) = \text{const}$. But the maximizing function will not, in general, obey $p(\theta) \geq 0$. Subject to this inequality $p_\star(\theta)$ must satisfy

$$\{p_\star(\theta) > 0,\, f_{\text{KL}}(\theta) = \text{MI}\} \text{ or } \{p_\star(\theta) = 0,\, f_{\text{KL}}(\theta) < \text{MI}\}$$

at every θ. With finite data $f_{\text{KL}}(\theta) - \text{MI}$ must be an analytic function of θ, and therefore must be smooth with a finite numbers of zeros, corresponding to the atoms of $p_\star(\theta)$ (Figure 1A). See (28, 29, 46) for related arguments for discreteness, and (41–43) for other approaches.

The number of atoms occurring in $p_\star(\theta)$ increases as the data improves. For K atoms there is an absolute bound $\text{MI} \leq \log K$, saturated if they are perfectly distinguishable. In Figure 2C we observe that the optimal priors instead approach a line $\text{MI} \to \zeta \log K$, with slope $\zeta \approx 0.75$. At large L the length of parameter space is proportional to the number of distinguishable points, hence $\text{MI} \to \log L$. Together these imply $K \sim L^{1/\zeta}$, and so the average number density of atoms grows as

$$\rho_0 = K/L \sim L^{1/\zeta - 1} \approx L^{1/3}, \qquad L \gg 1. \qquad [4]$$

¶ The function $f_{\text{KL}}(\theta)$ is sometimes called the Bayes risk, as it quantifies how poorly the prior will perform if θ turns out to be correct. One of the problems equivalent to maximising the mutual information (40) is the minimax problem for this (see also Figure 1):

$$\max_{p(\theta)} I(X; \Theta) = \min_{p(\theta)} \max_\theta f_{\text{KL}}(\theta) = \min_{q(x)} \max_{p(\theta)} \int d\theta p(\theta) D_{\text{KL}}\left[p(x|\theta)\|q(x)\right].$$

The distributions we call expected data $p(x)$ are also known as Bayes strategies, i.e. distributions on X which are the convolution of the likelihood $p(x|\theta)$ with some prior $p(\theta)$. The optimal $q(x)$ from this third formulation (with $\min_{q(x)} \ldots$) can be shown to be such a distribution (40).
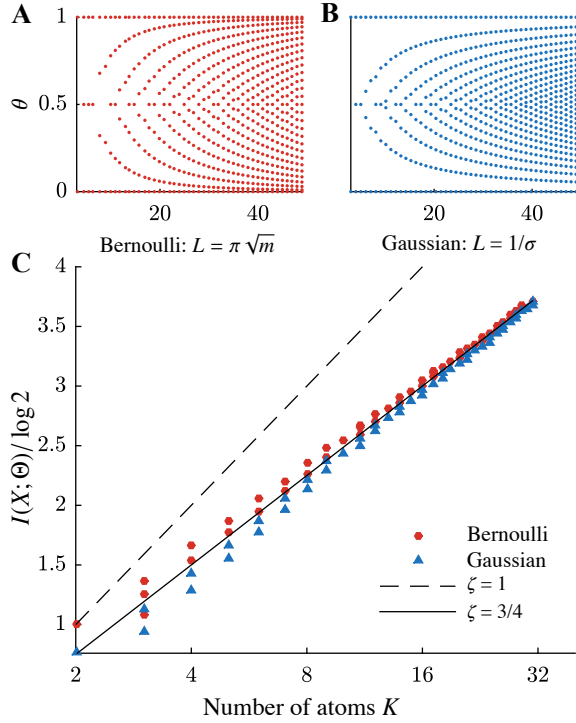
Mattingly, Transtrum, Abbott, Machta | Rational Ignorance

PNAS | **7 February, 2018** | vol. XXX | no. XX | **3**

Fig. 3. Behavior of $p_\star(\theta)$ with increasing Fisher length. Panels A and B show the atoms of $p_\star(\theta)$ for the two one-dimensional models as L is increased (i.e. we perform more repetitions m or have smaller noise σ). Panel C shows the scaling of the mutual information (in bits) with the number of atoms K. The dashed line is the bound $MI \leq \log K$, and the solid line is the scaling law $MI \sim 3/4 \log K$.

Thus the proper spacing between atoms shrinks to zero in the limit of infinite data, i.e. neighboring atoms cease to be distinguishable.

To derive this scaling law analytically, in a related paper (51) we consider a field theory for the number density of atoms, in which the entropy density (omitting numerical factors) is

$$\mathcal{S} = \text{const.} - e^{-\rho^2}[\rho^4(\rho')^2 + 1].$$

From this we find $\zeta = 3/4$, which is consistent with both examples presented above.

Multi-parameter Example

In the examples above, $p_\star(\theta)$ concentrates weight on the edges of its allowed domain when data is scarce (i.e. when m is small or σ is large, hence L is small). We next turn to a multi-parameter model in which some parameter combinations are ill-constrained, and where edges correspond to reduced models.

The physical picture is that we wish to determine the composition of an unknown radioactive source, from data of x_t Geiger counter clicks at some times t. As parameters we have the quantities A_μ and decay constants k_μ of isotopes μ. The probability of observing x_t should be a Poisson distribution (of mean y_t) at each time, but we approximate these by Gaussians to write:[||]

$$p(\vec{x}|\vec{y}) \propto \prod_t e^{-(x_t - y_t)^2/2\sigma^2}, \qquad y_t = \sum_\mu A_\mu e^{-k_\mu t}. \quad [5]$$

[||] Using a normal distribution of fixed σ here is what allows the metric in Eq. (6) to be so simple. However the qualitative behavior from the Poisson distribution is very similar.
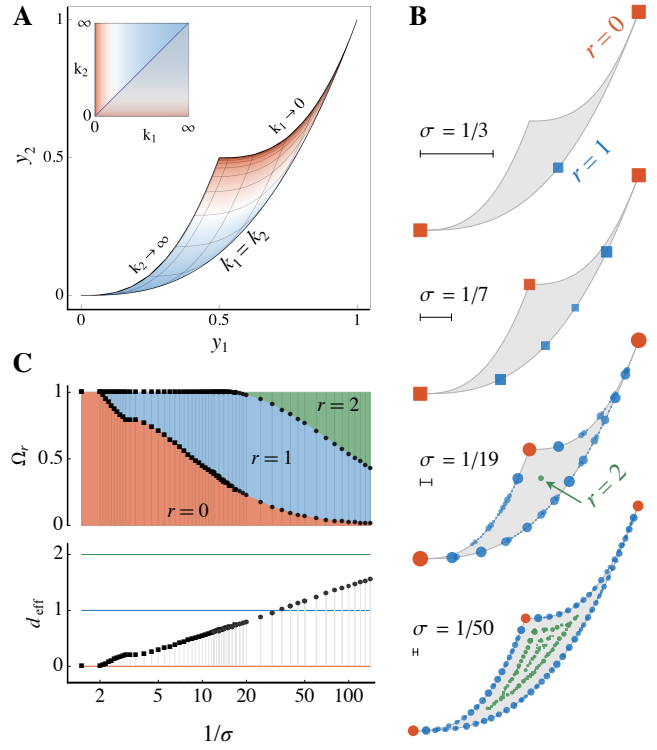

Fig. 4. Parameters and priors for the exponential model (5). Panel A shows the area of the $\vec{y}$ plane covered by all decay constants $k_1, k_2 \geq 0$. Panel B shows the positions of the delta functions of the optimal prior $p_\star(\vec{y})$ for several values of σ, with colors indicating the dimensionality r at each point. Panel C shows the proportion of weight on these dimensionalities.

Fixing $\sigma_t = \sigma = \text{const.}$ then brings us to a nonlinear least-squares model of the type studied by (6, 7). This same model also arises in other contexts, such as the asymptotic approach to equilibrium of many dynamical systems (52).

We can see the essential behavior with just two isotopes in fixed quantities: $A_\mu = \frac{1}{2}$, thus $y_t = \frac{1}{2}(e^{-k_1 t} + e^{-k_2 t})$. Measuring at only two times t_1 and t_2, we almost have a two-dimensional version of Eq. (2), in which the center of the distribution $\vec{y} = (y_1, y_2)$ plays the role of θ above. The mapping between $\vec{k}$ and $\vec{y}$ is shown in Figure 4A, fixing $t_2/t_1 = e$. The Fisher information metric is proportional to the ordinary Euclidean metric for $\vec{y}$, but not for $\vec{k}$:

$$g_{\mu\nu}(\vec{k}) = \frac{1}{\sigma^2}\sum_t \frac{\partial y_t}{\partial k_\mu}\frac{\partial y_t}{\partial k_\nu} \iff g_{st}(\vec{y}) = \frac{1}{\sigma^2}\delta_{st}. \quad [6]$$

Thus Jeffreys prior is a constant on the allowed region of the $\vec{y}$ plane.

Then we proceed to find the optimum $p_\star(\vec{y})$ for this model, shown in Figure 4B for various values of σ. When σ is large, this has delta functions only in two of the corners, allowing only $k_1, k_2 = 0$ and $k_1, k_2 = \infty$. As σ is decreased, new atoms appear first along the lower boundary (corresponding to the one-dimensional model where $k_1 = k_2$) and then along the other boundaries. At sufficiently small σ, atoms start filling in the (two-dimensional) interior.

To show this progression in Figure 4C, we define Ω_r as the total weight on all edges of dimension r, and an effective dimensionality $d_{\text{eff}} = \sum_{r=1}^{D} r\,\Omega_r$. This increases smoothly from 0 towards $D = 2$ as the data improves.
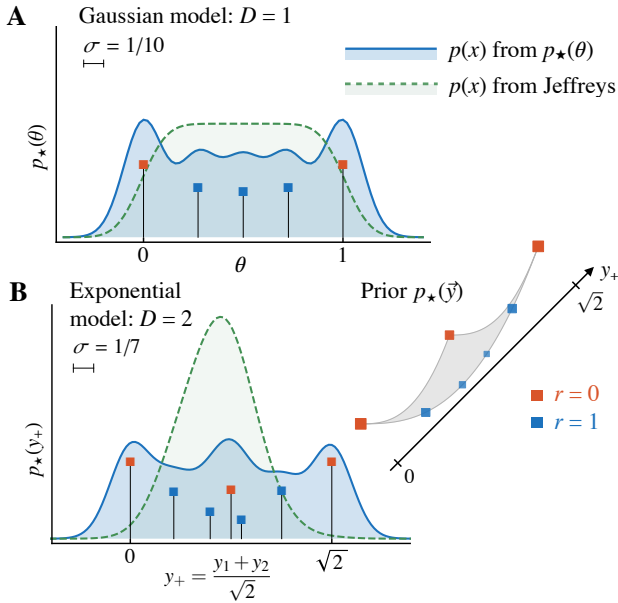
Fig. 5. Distributions of expected data $p(x)$ from different priors. Panel A is the one-parameter Gaussian model, with $L = 10$. Panel B projects the two-parameter exponential model onto the $y_1 + y_2$ direction, for $\sigma = 1/7$ where the perpendicular direction should be irrelevant. The length of the relevant direction is about the same as the one-parameter case: $L_+ = 7\sqrt{2}$. Notice that the distribution of expected data $p(x_+)$ from Jeffreys prior here is quite different, with almost no weight at the ends of the range (0 and $\sqrt{2}$), because this prior still weights the area not the length.

At medium values of σ, the prior $p_\star(\vec{y})$ almost ignores the width of the parameter manifold, and cares mostly about its length ($L_+ = \sqrt{2}/\sigma$ along the diagonal). This behavior is very different to that of Jeffreys prior: in Figure 5B we demonstrate this by plotting the distributions of data implied by these two priors. Jeffreys puts almost no weight near the ends of the long (i.e. stiff, or relevant) parameter's range, because the (sloppy, or irrelevant) width happens to be even narrower there than in the middle. By contrast our effective model puts significant weight on each end, much like the one-parameter model in Figure 5A.

The difference between one and two parameters being relevant (in Figure 4B) is very roughly $\sigma = 1/7$ to $\sigma = 1/50$, a factor 7 in Fisher length, thus a factor 50 in the number of repetitions m — perhaps the difference between a week's data and a year's. These numbers are artificially small to demonstrate the appearance of models away from the boundary: more realistic models often have manifold lengths spread over many orders of magnitude (5, 8), and thus have some parameters inaccessible even with centuries of data. To measure these we need a qualitatively different experiment, justifying a different effective theory.

The one-dimensional model along the lower edge of Figure 4A is the effective theory with equal decay constants. This remains true if we allow more parameters $k_3, k_4, \ldots$ in Eq. (5), and $p_\star(\vec{y})$ will still place a similar weight there.[**] Measuring x_t also at later times $t_3, t_4, \ldots$ will add more thin directions to the manifold (7), but the one-dimensional boundary corresponding

to equal decay constants will still have significant weight. The fact that such edges give human-readable simpler models (unlike arbitrary submanifolds) was the original motivation for preferring them in (22), and it is very interesting that our optimization procedure has the same preference.[††]

Discussion

While the three examples we have studied here are very simple, they demonstrate a principled way of selecting optimal effective theories, especially in high-dimensional settings. Following (45), we may call this rational ignorance.

The prior $p_\star(\theta)$ which encodes this selection is the maximally uninformative prior, in the sense of leaving maximum headroom for learning from data. But its construction depends on the likelihood function $p(x|\theta)$, and thus it contains knowledge about the experiment through which we are probing nature. Jeffreys prior $p_J(\theta)$ also depends on the experiment, but more weakly: it is independent of the number of repetitions m, precisely because it is the limit $m \to \infty$ of the optimal prior (32, 33).

Under either of these prescriptions, performing a second experiment may necessitate a change in the prior, leading to a change in the posterior not described by Bayes' theorem. If the second experiment is different from the first, then changing to Jeffreys prior for the combined experiment (and then applying Bayes' rule just once) will have this effect (56, 57).[‡‡] Our prescription differs from Jeffreys in also regarding more repetitions of an identical experiment as being different. Many experiments would have much higher resolution if they could be repeated for all eternity. The fact that they cannot is an important limit on the accuracy of our knowledge, and our proposal treats this limitation on the same footing as the rest of the specification of the experiment.

Keeping m finite is where we differ from earlier work on prior selection. Bernardo's reference prior (31) maximizes the same mutual information, but always in the $m \to \infty$ limit where it gives a smooth analytically tractable function. Using $I(X;\Theta)$ to quantify what can be learned from an experiment goes back to Lindley (24). That finite information implies a discrete distribution was known at least since (26, 27). What has been overlooked is that this discreteness is useful for avoiding a problem with Jeffreys prior on the hyper-ribbon parameter spaces generic in science (5): because it weights the irrelevant parameter volume, Jeffreys prior has strong dependence on microscopic effects invisible to experiment. The limit $m \to \infty$ has erased the divide between relevant and irrelevant parameters, by throwing away the natural length scale on the parameter manifold. By contrast $p_\star(\theta)$ retains discreteness at roughly this scale, allowing it to ignore irrelevant directions. Along a relevant parameter direction this discreteness is no worse than rounding θ to as many digits as we can hope to measure, and we showed that in fact the spacing of atoms decreases faster than our accuracy improves.

[**]If we have more parameters than measurements then the model must be singular. In fact the exponential model of Figure 4 is already slightly singular, since $k_1 \leftrightarrow k_2$ does not change the data; we could cure this by restricting to $k_2 \geq k_1$, or by working with $\vec{y}$, to obtain a regular model.

[††]Edges of the parameter manifold give simpler models not only in the sense of having fewer parameters, but also in an algorithmic sense. For example, the Michaelis–Menten model is analytically solvable (53) in a limit which corresponds to a manifold boundary (54). Stable linear dynamical systems of order n are model boundaries order $n + 1$ systems (55). Taking some parameter combinations to the extreme can lock spins into Kadanoff blocks (54).

[‡‡]This view is natural in the objective Bayesian tradition, but see (58) and (59–61) for alternative viewpoints.

Mattingly, Transtrum, Abbott, Machta | Rational Ignorance

PNAS | **7 February, 2018** | vol. XXX | no. XX | **5**

Model selection is more often studied not as part of prior selection, but at the stage of fitting the parameters to data. From noisy data, one is tempted to fit a model which is more complicated than reality; avoiding such overfitting improves predictions. The AIC, BIC (15, 62) and related criteria (19, 20, 63–65) are subleading terms of various measures in the $m \to \infty$ limit, in which all (nonsingular) parameters of the true model can be accurately measured. Techniques like MDL, NML, and cross-validation (63, 66, 67) need not take this limit, but all are applied after seeing the data. They favor minimally flexible models close to the data seen, while our procedure favors one answer which can distinguish as many different outcomes as possible. It is curious that both approaches can point towards simplicity. We explore this contrast in more detail in the Appendix.§§

Being discrete, the prior $p_\star(\theta)$ is very likely to exclude the true value of the parameter, if such a $\theta_{\text{true}} \in \Theta$ exists. This is not a flaw: the spirit of effective theory is to focus on what is relevant for describing the data, deliberately ignoring microscopic effects which we know to exist (68). Thus the same effective theory can emerge from different microscopic physics [as in the universality of critical points describing phase transitions (69)]. The relevant degrees of freedom are often quasiparticles [such as the Cooper pairs of superconductivity (70)] which do not exist in the microscopic theory, but give a natural and simple description at the scale being observed. We argued here for such simplicity not on the grounds of the difficulty of simulating 10^{23} electrons, nor of human limitations, but based on the natural measure of information learned.

There is similar simplicity to be found outside of physics. For example the Michaelis–Menten law for enzyme kinetics (71) is derived as a limit in which only the ratios of some reaction rates matter, and is useful regardless of the underlying system. In more complicated systems which we cannot solve by hand, and for which the symmetries and scaling arguments used in physics cannot be applied, we hope that our information approach may be useful for identifying the appropriately detailed theory.

1. L. P. Kadanoff, *Scaling laws for Ising models near T_c*, Physics **2** (1966) 263–272.
2. K. G. Wilson, *Renormalization group and critical phenomena. 1. Renormalization group and the Kadanoff scaling picture*, Phys. Rev. **B4** (1971) 3174–3183.
3. J. L. Cardy, *Scaling and renormalization in statistical physics*. Cambridge Univ. Press, 1996.
4. J. J. Waterfall, F. P. Casey, R. N. Gutenkunst, K. S. Brown, C. R. Myers, P. W. Brouwer and J. P. Sethna, *Sloppy-model universality class and the Vandermonde matrix.*, Phys. Rev. Lett. **97** (2006) 150601–4.
5. R. N. Gutenkunst, J. J. Waterfall, F. P. Casey, K. S. Brown, C. R. Myers and J. P. Sethna, *Universally Sloppy Parameter Sensitivities in Systems Biology Models*, PLoS Comp. Biol. **3** (2007) e189–8.

6. M. K. Transtrum, B. B. Machta and J. P. Sethna, *Why are Nonlinear Fits to Data so Challenging?*, Phys. Rev. Lett. **104** (2010) 060201 [arXiv:0909.3884].
7. M. K. Transtrum, B. B. Machta and J. P. Sethna, *Geometry of nonlinear least squares with applications to sloppy models and optimization*, Phys. Rev. **E83** (2011) 036701 [arXiv:1010.1449].
8. B. B. Machta, R. Chachra, M. K. Transtrum and J. P. Sethna, *Parameter Space Compression Underlies Emergent Theories and Predictive Models*, Science **342** (2013) 604–607 [arXiv:1303.6738].
9. M. K. Transtrum, B. B. Machta, K. S. Brown, B. C. Daniels, C. R. Myers and J. P. Sethna, *Perspective: Sloppiness and emergent theories in physics, biology, and beyond*, J. Chem. Phys. **143** (2015) 010901 [arXiv:1501.07668].
10. T. O'Leary, A. C. Sutton and E. Marder, *Computational models in the age of large datasets*, Cur. Op. Neurobio. **32** (2015) 87–94.
11. T. Niksic and D. Vretenar, *Sloppy nuclear energy density functionals: effective model reduction*, Phys. Rev. **C94** (2016) 024333 [arXiv:1606.08617].
12. D. V. Raman, J. Anderson and A. Papachristodoulou, *Delineating Parameter Unidentifiabilities in Complex Models*, arXiv:1607.07705.
13. G. Bohner and G. Venkataraman, *Identifiability, reducibility, and adaptability in allosteric macromolecules*, J. Gen. Physiol. **149** (2017) 547–560.
14. A. Raju, B. B. Machta and J. P. Sethna, *Information geometry and the renormalization group*, arXiv:1710.05787.
15. H. Akaike, *A new look at the statistical model identification*, IEEE Trans. Automat. Contr. **19** (1974) 716–723.
16. N. Sugiura, *Further analysts of the data by Akaike's information criterion and the finite corrections*, Comm. Stat. Th. Meth. **7** (1978) 13–26.
17. V. Balasubramanian, *Statistical inference, Occam's razor, and statistical mechanics on the space of probability distributions*, Neural Comp. **9** (1997) 349–368.
18. I. J. Myung, V. Balasubramanian and M. A. Pitt, *Counting probability distributions: differential geometry and model selection.*, PNAS **97** (2000) 11170–11175.
19. D. J. Spiegelhalter, N. G. Best, B. P. Carlin and A. Van Der Linde, *Bayesian measures of model complexity and fit*, J. Roy. Stat. Soc. B **64** (2002) 583–639.
20. S. Watanabe, *Asymptotic equivalence of Bayes cross validation and widely applicable information criterion in singular learning theory*, JMLR **11** (2010) 3571–3594 [arXiv:1004.2316].
21. P. A. Wiggins and C. H. LaMont, *Information-based inference for singular models and finite sample sizes*, arXiv:1506.05855.
22. M. K. Transtrum and P. Qiu, *Model reduction by manifold boundaries*, Phys. Rev. Lett. **113** (2014) 098701–6.
23. C. E. Shannon, *A mathematical theory of communication*, Bell Sys. Tech. J. **27** (1948) 623–656.
24. D. V. Lindley, *On a Measure of the Information Provided by an Experiment*, Ann. Math. Statist. **27** (1956) 986–1005.
25. A. Rényi, *On some basic problems of statistics from the point of view of information theory*, Proc. 5th Berkeley Symp. on Math. Statist. and Prob. (1967) 531–543. [projecteuclid.org].
26. G. Färber, *Die Kanalkapazität allgemeiner Übertragunskanäle bei begrenztem Signalwertbereich beliebigen Signalübertragungszeiten sowie beliebiger Störung*, Arch. Elektr. Übertr. **21** (1967) 565–574.
27. J. G. Smith, *The information capacity of amplitude-and variance-constrained scalar gaussian channels*, Information and Control **18** (1971) 203–219.
28. S. L. Fix, *Rate distortion functions for squared error distortion measures*, Proc. 16th Annu. Allerton Conf. Commun. Control Comput. (1978) 704–711.
29. J. O. Berger, J. M. Bernardo and M. Mendoza, *On Priors that Maximize Expected Information*, Recent Developments in Statistics and Their Applications (1988) 1–20. [www.uv.es/~bernardo/].
30. Z. Zhang, *Discrete Noninformative Priors*. PhD thesis, Yale University, 1994. [UMI 9523257].
31. J. M. Bernardo, *Reference Posterior Distributions for Bayesian Inference*, J. Roy. Stat. Soc. B **41** (1979) 113–147. [www.uv.es/~bernardo/].
32. B. S. Clarke and A. R. Barron, *Jeffreys' prior is asymptotically least favorable under entropy risk*, J. Stat. Plan. Infer. **41** (1994) 37–60.
33. H. R. Scholl, *Shannon optimal priors on independent identically distributed statistical experiments converge weakly to Jeffreys' prior*, Test **7** (1998) 75–94.
34. H. Jeffreys, *An Invariant Form for the Prior Probability in*

---

§§Model selection usually starts from a list of models to be compared, in our language a list of submanifolds of Θ. We can also consider maximising mutual information in this setting, rather than with an unconstrained function $p(\theta)$, and unsurprisingly we observe a similar preference for highly flexible simpler models. This is also discussed in the Appendix, at Eq. (S3).

Estimation Problems, Proc. Roy. Soc. A **186** (1946) 453–461.

35. J. E. Kerrich, *An Experimental Introduction to the Theory of Probability.* Copenhagen: E Munksgaard, 1946.

36. C. O'Luanaigh, *CERN data centre passes 100 petabytes*, home.cern (2013).

37. S. Arimoto, *An algorithm for computing the capacity of arbitrary discrete memoryless channels*, IEEE Trans. Inform. Theory **18** (1972) 14–20.

38. R. Blahut, *Computation of channel capacity and rate-distortion functions*, IEEE Trans. Inform. Theory **18** (1972) 460–473.

39. K. Rose, *A mapping approach to rate-distortion computation and analysis*, IEEE Trans. Inform. Theory **40** (1994) 1939–1952.

40. D. Haussler, *A general minimax result for relative entropy*, IEEE Trans. Inform. Theory **43** (1997) 1276–1280.

41. M. N. Ghosh, *Uniform Approximation of Minimax Point Estimates*, Ann. Math. Statist. **35** (1964) 1031–1047.

42. G. Casella and W. E. Strawderman, *Estimating a Bounded Normal Mean*, Ann. Statist. **9** (1981) 870–878.

43. I. Feldman, *Constrained Minimax Estimation of the Mean of the Normal Distribution with Known Variance*, Ann. Statist. **19** (1991) 2259–2265.

44. M. Chen, D. Dey, P. Müller, D. Sun and K. Ye, *Frontiers of statistical decision making and Bayesian analysis.* Springer, New York, NY, 2010.

45. C. A. Sims, *Rational Inattention: Beyond the Linear-Quadratic Case*, American Economic Review **96** (2006) 158–163.

46. J. Jung, J. Kim, F. Matějka and C. A. Sims, *Discrete Actions in Information-Constrained Decision Problems*, . [princeton.edu/~sims/#RIDiscrete].

47. S. Laughlin, *A simple coding procedure enhances a neuron's information capacity*, Z. Naturforsch. **36 c** (1981) 910–912.

48. G. Tkačik, C. G. Callan and W. Bialek, *Information flow and optimization in transcriptional regulation*, PNAS **105** (2008) 12265–12270 [arXiv:0705.0313].

49. M. D. Petkova, G. Tkačik, W. Bialek, E. F. Wieschaus and T. Gregor, *Optimal decoding of information from a genetic network*, arXiv:1612.08084.

50. A. Mayer, V. Balasubramanian, T. Mora and A. M. Walczak, *How a well-adapted immune system is organized*, PNAS **112** (2015) 5950–5955 [arXiv:1407.6888].

51. M. C. Abbott and B. B. Machta, *An information scaling law: ζ = 3/4*, arXiv:1710.09351.

52. S. H. Strogatz, *Nonlinear Dynamics And Chaos.* Sarat Book House, 2007.

53. S. Schnell and C. Mendoza, *Closed Form Solution for Time-dependent Enzyme Kinetics*, J. Theor. Biol. **187** (1997) 207–212.

54. M. Transtrum, G. Hart and P. Qiu, *Information topology identifies emergent model classes*, arXiv:1409.6203.

55. P. E. Paré, A. T. Wilson, M. K. Transtrum and S. C. Warnick, *A unified view of Balanced Truncation and Singular Perturbation Approximations*, in *Proceedings of the American Control Conference*, pp. 1989–1994, IEEE, 2015.

56. N. Lewis, *Combining independent Bayesian posteriors into a confidence distribution, with application to estimating climate sensitivity*, J. Stat. Plan. Infer. (2017) to appear.

57. N. Lewis, *Modification of Bayesian Updating where Continuous Parameters have Differing Relationships with New and Existing Data*, arXiv:1308.2791.

58. D. Poole and A. E. Raftery, *Inference for Deterministic Simulation Models: The Bayesian Melding Approach*, J. Amer. Stat. Assoc. **95** (2000) 1244–1255.

59. T. Seidenfeld, *Why I am not an objective Bayesian; some reflections prompted by Rosenkrantz*, Theor Decis **11** (1979) 413–440.

60. R. E. Kass and L. Wasserman, *The selection of prior distributions by formal rules*, J. Amer. Stat. Assoc. **91** (1996) 1343–1370.

61. J. Williamson, *Objective Bayesianism, Bayesian conditionalisation and voluntarism*, Synthese **178** (2009) 67–85.

62. G. Schwarz, *Estimating the dimension of a model*, Ann. Statist. **6** (1978) 461–464.

63. J. Rissanen, *Modeling by Shortest Data Description*, Automatica **14** (1978) 465–471.

64. C. S. Wallace and D. M. Boulton, *An Information Measure for Classification*, The Computer Journal **11** (1968) 185–194.

65. S. Watanabe, *A widely applicable Bayesian information criterion*, JMLR **14** (2013) 867–897 [arXiv:1208.6338].

66. P. D. Grünwald, I. J. Myung and M. A. Pitt, *Advances in Minimum Description Length: Theory and Applications.* 2009.

67. S. Arlot and A. Celisse, *A survey of cross-validation procedures for model selection*, Statistics Surveys **4** (2010) 40–79.

68. P. W. Anderson, *More Is Different*, Science **177** (1972) 393–396.

69. R. W. Batterman, *Philosophical Implications of Kadanoff's Work on the Renormalization Group*, J. Stat. Phys. **167** (2017) 559–574. [pitt.edu/~rbatterm/].

70. J. Bardeen, L. N. Cooper and J. R. Schrieffer, *Theory of superconductivity*, Phys. Rev. **108** (1957) 1175–1204.

71. L. Michaelis and M. L. Menten, *The kinetics of invertin action*, FEBS Letters **587** (2013) 2712–2720. [Translation by T. R. C. Boyde].

72. R. E. Kass and A. E. Raftery, *Bayes Factors*, J. Amer. Stat. Assoc. **90** (1995) 773.

73. A. Bhadra, J. Datta, N. G. Polson and B. Willard, *Default Bayesian analysis with global-local shrinkage priors*, Biometrika **103** (Dec., 2016) 955–969.

74. D. Simpson, H. Rue, A. Riebler and T. G. Martins, *Penalising Model Component Complexity: A Principled, Practical Approach to Constructing Priors*, Statist. Sci. **32** (2017) 1–28 [arXiv:1403.4630].

75. J. I. Myung, D. J. Navarro and M. A. Pitt, *Model selection by normalized maximum likelihood*, Journal of Mathematical Psychology **50** (2006) 167–179.

76. P. D. Grünwald, *The Minimum Description Length Principle.* MIT Press, 2007.

77. C.-I. Chang and L. D. Davisson, *On calculating the capacity of an infinite-input finite (infinite)-output channel*, IEEE Trans. Inform. Theory **34** (1988) 1004–1010.

78. J. Lafferty and L. Wasserman, *Iterative Markov chain Monte Carlo computation of reference priors and minimax risk*, Proc. 17th conf. Uncert. AI (2001) 293–300 [arXiv:1301.2286].

79. J. Dauwels, *Numerical computation of the capacity of continuous memoryless channels*, Proc. 26th Symp. Inf. Th. Benelux (2005). [www.dauwels.com].

Appendix: Model Selection from Data

The usual discussion of model selection takes place after observing data x. If we wish to compare some models[*] labeled by d, each with some prior $p_d(\theta)$, then one prescription is to choose the model with the largest $p(x)$. Labelling this explicitly, we write

$$p(x|d) = \int_{\Theta_d} d\theta \, p(x|\theta) \, p_d(\theta), \qquad p_d(\theta) > 0 \text{ on } \Theta_d \subset \Theta. \quad [\text{S1}]$$

If the Bayes factor $p(x|d)/p(x|d')$ is larger than one then (absent any other information) d is preferred over d' (72).[†] In the usual asymptotic limit $m \to \infty$, this idea leads to minimising the Bayesian information criterion (BIC) (62):

$$-\log p(x|d) \approx -\log p(x|\hat{\theta}_d) + \frac{d}{2} \log m + \mathcal{O}(m^0)$$

where $-\log p(x|\hat{\theta}_d) = \frac{1}{2}\chi^2 = \frac{1}{2}\sum_{i=1}^{m}[x_i - y_i(\hat{\theta}_d)]^2/\sigma^2 \sim \mathcal{O}(m)$, and $\hat{\theta}_d$ is a maximum likelihood estimator for x, constrained to the appropriate subspace:

$$\hat{\theta}_d(x) = \operatorname*{argmax}_{\theta \in \Theta_d} p(x|\theta).$$

The term $d \log m$ penalises models with more parameters, even though they can usually fit the data more closely. Despite the name this procedure is not very Bayesian: one chooses the effective model (and hence the prior) after seeing the data, rather than simply updating according to Bayes theorem.[‡]

---

[*] The word model unfortunately means several things in the literature. We mean parameter space Θ_d always equipped with a likelihood function $p(x|\theta)$, and usually with a prior $p_d(\theta)$. When this is a subspace of some larger model Θ_D (whose likelihood function agrees, but whose prior may be unrelated) then we term the smaller one an effective model, or a reduced model, although we do not always write the adjective. The optimal prior $p_\star(\theta)$ defines an effective model in this sense. Its support will typically be on several boundaries of Θ_D. If the boundaries of Θ_D (of all dimensions) are regarded as a canonical list of reduced models, then $p_\star(\theta)$ is seldom a sub-model of any one of them.

[†] If one of the priors is improper, say $\int d\theta \, p_d(\theta) = \infty$, then $p(x|d)$ will also be infinite. In this sense the Bayes factor behaves worse than the posterior $p(\theta|x)$, which can still be finite.

[‡] Terms penalising more complex models can be translated into shrinkage priors, which concentrate weight near to simpler models (73). Perhaps the shrinkage priors closest
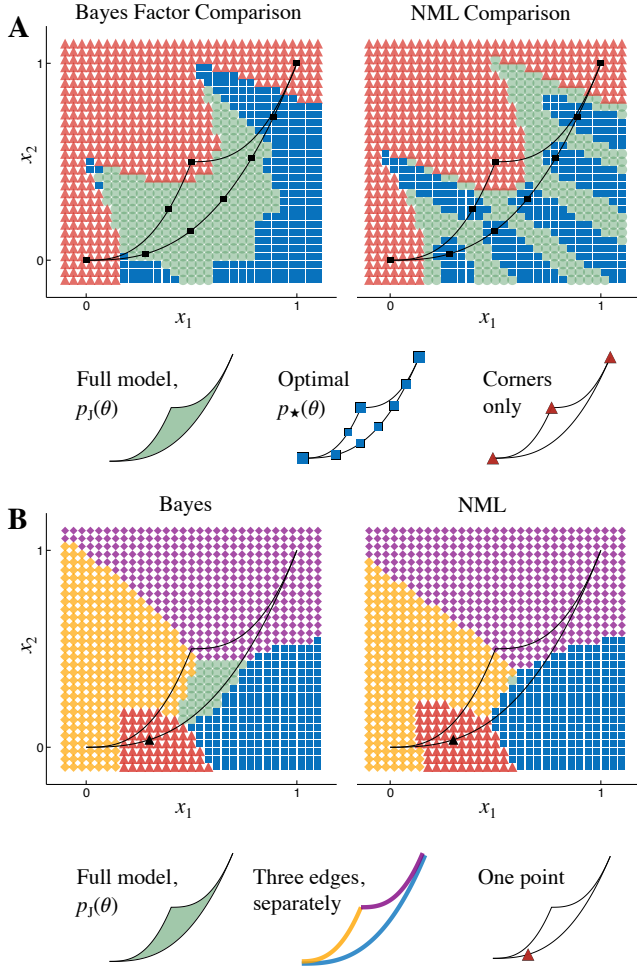
Mattingly, Transtrum, Abbott, Machta | Rational Ignorance

PNAS | **7 February, 2018** | vol. XXX | no. XX | **7**

Related prescriptions can be derived from minimum description length (MDL) ideas. To allow reconstruction of the data we transmit both the fitted parameters and the residual errors, and minimising the (compressed) length of this transmission drives a tradeoff between error and complexity (63, 64, 66). A convenient version of this goes by the name of normalized maximum likelihood (NML) (75, 76), and chooses the model d which maximizes

$$p_d^{\mathrm{NML}}(x) = \frac{p\big(x|\hat{\theta}_d(x)\big)}{Z_d}, \qquad Z_d = \int_{\Theta_d} dx'\, p\big(x'|\hat{\theta}_d(x')\big). \quad [\mathrm{S2}]$$

This is not Bayesian in origin, and does not depend on the prior on each effective model d, only its support Θ_d. The function $p_d^{\mathrm{NML}}(x)$ is not expected data in the sense of $p(x)$ — it is not the convolution of the likelihood with any prior.[§] In the asymptotic limit $p_d^{\mathrm{NML}}(x)$ approaches $p(x)$ from Jeffreys prior, and this criterion agrees with BIC (63), but away from this limit they differ.

In Figure S1 we apply these two prescriptions to the exponential example treated in the text. At each $\vec{x} \in X$ we indicate which of a list of models is preferred.[¶] Figure S2 instead draws the distributions being used.

- Figure S1A compares three models: the complete model (with Jeffreys prior), the optimal model described by discrete prior $p_\star(\vec{y})$, and an even simpler model with weight only on the three vertices $\vec{y} = (0,0)$, $(\frac{1}{2}, \frac{1}{2})$, $(1,1)$.
- Figure S1B instead compares the complete model to three different one-parameter models (along the three boundaries of the allowed region of the $\vec{y}$ plane) and a zero-parameter model (one point $\vec{y}$, in no particularly special place). In terms of decay rates the three lines are limits $k_1 = k_2$, $k_1 = 0$ and $k_2 = \infty$.

Different effective models are preferred for different values of data x. At a given point x, if several models contain the same $\hat{\theta}(x)$ then the simplest among them is preferred, which in the NML case means precisely the one with the smallest denominator Z_d. In fact a trivial model consisting of just one point $\Theta_0 = \hat{\theta}(x)$ would always be preferred if it were among those considered — there is no automatic preference for models which can produce a wide range of possible data.

By contrast our prior selection approach aims to be able to distinguish as many possible outcomes in X as possible. Applied to the same list of models as in Figure S1, this gives the following fixed scores (base e):

$$I_{\mathrm{full}} = 1.296, \qquad I_\star = 1.630, \qquad I_{\mathrm{corners}} = 1.098$$

and

$$\begin{aligned} I_{\mathrm{upper}} &= 0.852, \qquad I_{\mathrm{lower\text{-}left}} = 0.845, \\ I_{\mathrm{lower\text{-}right}} &= 1.418, \qquad I_{\mathrm{one\text{-}point}} = 0. \end{aligned} \quad [\mathrm{S3}]$$

Fig. S1. Model selection from data point x. Each large panel here shows which of a list of effective models is preferred after observing data $x \in X$. On the left the criterion is maximizing Eq. (S1), on the right the criterion is Eq. (S2). We study the same exponential model considered above, with $\sigma = 1/10$. Panel A compares our optimal effective model with prior $p_\star(\theta)$ to the full model (with Jeffeys prior) and to an even simpler model whose prior is just three delta functions. (These are drawn in the legend below). Panel B compares the full model to three different one-dimensional models, each allowing only one edge of Θ (with a uniform prior along this, i.e. the one-dimensional Jeffreys prior) and also to a trivial model (just one point), again with colors as indicated just below.

to this paper's are the penalised complexity priors of (74). Those are also reparameterization invariant, and also concentrate weight on a subspace of Θ, often a boundary. However both the subspace (or base model) and the degree of concentration (scaling parameter) are chosen by hand, rather than being deduced from $p(x|\theta)$.

[§]This relevant optimization problem here can be described as minimizing worst-case expected regret, written (75)

$$p_d^{\mathrm{NML}} = \underset{q}{\mathrm{argmin}}\ \underset{x}{\max}\ \log \frac{p(x|\hat{\theta}_d(x))}{q(x)}, \qquad \hat{\theta}_d(x) \in \Theta_d.$$

Perhaps the closest formulation of our maximum mutual information problem is that our $p_\star(x)$, the distribution on X not the prior, can be found as follows (40):

$$p_\star = \underset{q \in B}{\mathrm{argmin}}\ \underset{\theta}{\max} \int_X dx\, p(x|\theta) \log \frac{p(x|\theta)}{q(x)}$$

where $q(x)$ is constrained to be a Bayes strategy i.e. to arise from some prior $p_\star(\theta)$. Note the absence of $\hat{\theta}_d(x)$ and the presence of an integral over X, corresponding to the fact thats that this maximization takes place without being given a subspace Θ_d nor seeing data x. The resulting distributions on X are also different, as drawn in Figure S2. If plotted on Figure 5B, $p_2^{\mathrm{NML}}(x)$ from the full model would be somewhere between the two expected data $p(x)$ lines there. But it is not a comparable object; its purpose is model comparison as in Figure S1.

[¶]Recall that $\vec{x}$ is $\vec{y}$ corrupted by Gaussian noise, and $\vec{y}$ is constrained to the area show in Figure 4A because it arises from decay rates k_μ via Eq. (5). We may regard either y_t or k_μ as being the parameters, generically θ.

Mattingly, Transtrum, Abbott, Machta | Rational Ignorance

A

$p(x|d)$

$p_d^{\text{NML}}(x)$

$d =$
- - - - Full model
——— Optimal $p_\star(\theta)$
········· Corners only
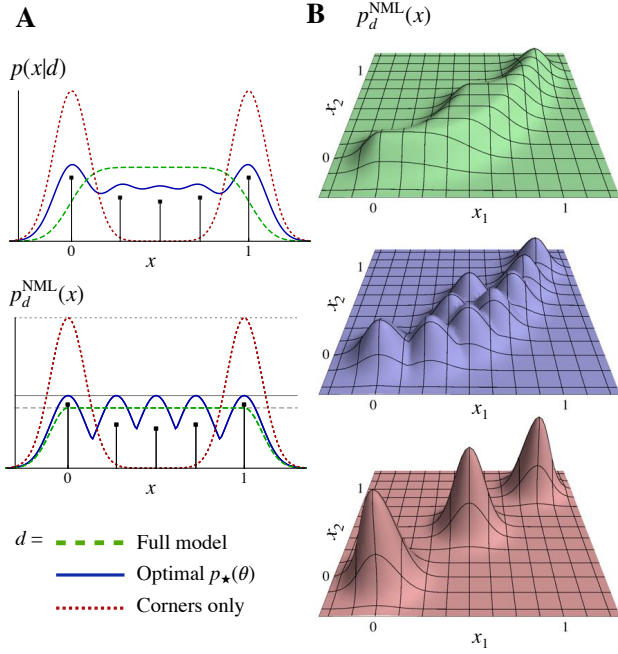
B $\quad p_d^{\text{NML}}(x)$

Fig. S2. Distributions over X. Panel A shows $p(x|d)$ Eq. (S1) and $p_d^{\text{NML}}(x)$ Eq. (S2) for the one-parameter Gaussian example Eq. (2) with $\sigma = 1/10$. The three models being compared are the full model (with a flat prior), the simpler model defined by $p_\star(\theta)$, and a model with just the endpoints of the line. Under the Bayes factor comparison, the $p_\star(\theta)$ model would never be preferred here. Panel B draws $p_d^{\text{NML}}(x)$ for the two-parameter exponential model, Eq. (5), for the complete model, the effective model defined by the support of $p_\star(\theta)$, and an even simpler model allowing only three points — the same three models as compared in Figure S1A. Notice that $p_d^{\text{NML}}(x)$ is always a constant on the allowed region $x \in y(\Theta_d)$.

By definition $p_\star(\theta)$ has the highest score. In second place comes the line along the lower edge (corresponding to $k_1 = k_2$). The shorter lines are strongly disfavored, because they cover a much smaller range of possible data.

Algorithms

The standard algorithm for maximizing channel capacity (of discrete memoryless channels) was written down independently by Blahut (38) and Arimoto (37). This aspect of rate-distortion theory is mathematically the same as the problem we consider, of maximizing mutual information by choosing the prior. The algorithm starts with $p_0(\theta) = $ const., and then at each time step updates this by

$$p_{\tau+1}(\theta) = \frac{1}{Z_\tau} e^{f_{\text{KL}}(\theta)} p_\tau(\theta) \qquad [\text{S4}]$$

where $Z_\tau = \int d\theta' \, e^{f_{\text{KL}}(\theta')} p_\tau(\theta')$ maintains normalization, and $f_{\text{KL}}(\theta) = D_{\text{KL}} [p(x|\theta) \| p(x)]$ is computed with $p_\tau(\theta)$. Since this
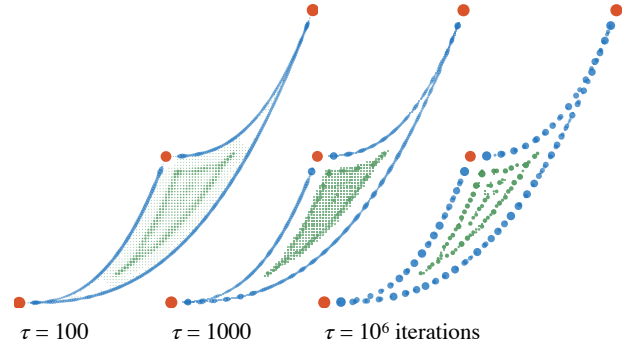

$\tau = 100 \qquad \tau = 1000 \qquad \tau = 10^6$ iterations

Fig. S3. Convergence of the BA algorithm (S4) for the exponential model. This shows $p_\star(\vec{y})$ for the case $\sigma = 1/50$, with $\vec{y}$ discretized on a grid of spacing $1/100$ in the bulk and $1/200$ along the boundaries of the allowed region.

is a convex optimization problem, the algorithm is guaranteed to converge to the global maximum. This makes it a good tool to see discreteness emerging.

Figures 2 and S3 show the progress of this algorithm for the one- and two-dimensional models in the text. We stress that the number and positions of the peaks which form are unchanged when the discretization of θ is made much finer. Notice also that the convergence to delta functions happens much sooner near to the boundaries than in the interior. The convergence to the correct mutual information $I(X; \Theta)$, and towards the optimum distribution on data space $p(x)$, happens much faster than the convergence to the correct number of delta functions.

Because θ must be discretized for this procedure, it is poorly suited to high-dimensional parameter spaces. However once we know that $p_\star(\theta)$ is discrete it is natural to consider algorithms exploiting this. With K atoms, we can adjust their positions $\vec{\theta}_a$ and weights λ_a using gradients

$$\frac{\partial \text{MI}}{\partial \theta_a^\mu} = \lambda_a \int dx \, \frac{\partial p(x|\vec{\theta})}{\partial \theta^\mu} \, \log \frac{p(x|\vec{\theta})}{p(x)} \bigg|_{\vec{\theta} = \vec{\theta}_a}$$

$$\frac{\partial \text{MI}}{\partial \lambda_a} = f_{\text{KL}}(\vec{\theta}_a) - 1. \qquad [\text{S5}]$$

Figures 1, 2A, 5 and the square plot points in Figure 4 were generated this way. This optimization is not a convex problem (there is some tendency to place two atoms on top of each other, and thus use too few points of support) but it can often find the optimum solution. We can confirm this by calculating $f_{\text{KL}}(\theta)$ everywhere — any points for which this is larger than its value at the atoms indicates that we do not have the optimal solution, and should add an atom.

Monte Carlo algorithms for this problem have been investigated in the literature, see (77, 78) and especially (79). (Incidentally, we observe that (77)'s table 1 contains a version of scaling law Eq. (4), with $\zeta \approx 1/2$. No attempt was made there to use the optimal number of atoms, only to calculate the channel capacity to sufficient accuracy.)